

# Efficient autofocus method for sequential automatic capturing of high-magnification microscopic images

Santiago Tello-Mijares<sup>1,2,3\*</sup>, Francisco Flores<sup>1</sup>, Jesús Bescós<sup>2</sup>, and Edgar Valdez<sup>3</sup>

<sup>1</sup>Instituto Tecnológico de la Laguna, Blvd. Revolución y Czda. Cuauhtemoc S/N CP 27000, Torreón, México

<sup>2</sup>VPU Lab, Escuela Politécnica Superior, Universidad Autónoma de Madrid, Ciudad Universitaria de Cantoblanco, 28049 Madrid, Spain

<sup>3</sup>EIIP Lab, Instituto Tecnológico Superior de Lerdo, Av. Tecnológico N° 1555 Placido Domingo, 35150, Lerdo, México

\*Corresponding author: s.tello@uam.es

Received March 23, 2013; accepted October 17, 2013; posted online December 5, 2013

This letter presents an autofocus (AF) method to position a high-magnification microscope lens that automatically captures hundreds of images from a single moving slide. These images are taken by a mobile clinic unit in a rural location, and are later automatically processed and revised by a remote specialist. This process requires high focus precision to enable image processing techniques to achieve proper results. Low focusing times are also required for the system to be operative. We propose a novel method that combines two focus measures with an adapted searching scheme to cope with both constraints.

OCIS codes: 110.0180, 110.2960, 100.2960.

doi: 10.3788/COL201311.121102.

Correct focus is an essential quality feature for images acquired as part of an artificial vision system<sup>[1]</sup>, as well as a critical step in the automatic capturing of microscopic images<sup>[2]</sup>. The context of this work is to develop a system that automatically captures hundreds of images from a provided slide sample in a rural location, selects images representing a sufficient number of cell nuclei, and sends them to a remote urban site for diagnosis. In this study, we target the automatic sequential capturing of hundreds of Pap smear images from a moving single microscope slide to obtain data for a particularly active field<sup>[3]</sup>.

When operating microscopes with lenses with over 40× magnification, the relative position between the lens and the smear should be set precisely to ensure that the object being observed or analyzed would be sharply perceived, thus requiring an autofocus (AF) method<sup>[4]</sup>. If such operation has to be performed automatically hundreds of times in large magnifications, then the efficiency and precision of the AF method are critical.

An AF method involves two operations: 1) a measure of the focus level on an image that is evaluated as a function of the lens position, thus generating a focus function (FF); 2) a searching algorithm that moves the lenses that are attempting to find the maximum FF<sup>[5]</sup> (Fig. 1). AF systems have been widely discussed in Ref. [1,2,4-22]. Reports have dealt either with evaluating focus measures<sup>[1,2,6,7,10-15,18,19]</sup> or determining optimal AF algorithms<sup>[4,5,8,9,16,17,20-22]</sup>. Some of these reports have focused on microscopic images<sup>[1,2,6,7,10,11,18,19]</sup>. These studies have all considered lenses moving along the  $z$  axis, but none has discussed lens scanning in the  $xy$  axis to capture images sequentially.

One of the most analyzed problems in AF methods is the presence of local maxima or minima in the FF, typically as a result of noise. In the microscopic image domain, two specific problems can be identified. The first

issue is a search algorithm that moves the lens back to a position declared as the maximum focus to capture the

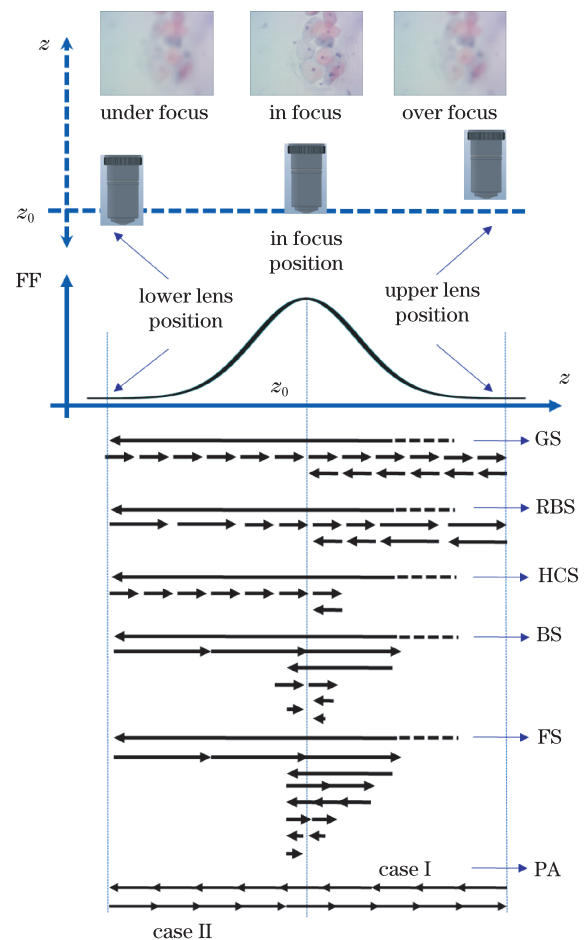


Fig. 1. (Color online) Evolution of the lens motion for the six analyzed searching algorithms.

best focused image. This process typically leads to focus imprecision because of the effect of vibration in high-magnification midrange setups. The second problem is search algorithms that require starting at a predefined out-of-focus position. These algorithms are inefficient if hundreds of images have to be captured sequentially from the same slide.

We propose a novel AF method to address these problems. The method uses a combination of measures to reduce noise. In addition, we propose a search mechanism to avoid moving lenses back and repositioning them for each captured image. Together, these features are crucial for a targeted application that automatically captures hundreds of images from a moving single slide. The proposed method then applies image processing techniques (which are highly sensitive to focus) to select and send these images for later analysis by a remote specialist.

In this letter, we present a comparison of 18 AF methods applied to microscopic images. We select two representative focus measures as well as the combination of these measures. The first measure is based on the image normalized variance (NV), whereas the second is a novel measure based on a discrete cosine transform (DCT). The top five search-based AF algorithms, namely, global search (GS), rule-based search (RBS), hill-climbing search (HCS), binary search (BS), and Fibonacci search (FS), are also considered along a proposed method. We combine these three focus measures and six algorithms, and compare them in an experiment.

The reported focus measures or functions include image differentiation, deep peaks and valleys, image contrast (statistical approaches) based on the histogram, and correlation measurements<sup>[1,6,7]</sup>. According to the domain, focus measures can also be divided into spatial and frequency measures. The former include Laplacian, Sobel, and statistical approaches that can determine sharpness with respect to the edge information or gradient magnitude of the image. The latter, such as a fast Fourier transform, a DCT, or a discrete wavelet transform, can determine sharpness by evaluating the high-frequency components of images<sup>[8]</sup>.

In the present work, we propose to analyze the behavior of the two best reported measures in the spatial and frequency domains: the NV and a DCT-based measure. Both measures lead to FFs with desirable properties such as: 1) their maximum value corresponds to the best focusing position, 2) they present almost no local maxima and noise, and 3) they are robust to the texture of the target object<sup>[9]</sup>. We also propose a combination of both measures.

NV: This basic statistical function evaluates image luminance variance relative to its mean value. In Ref. [10], 11 FFs were evaluated on an electron microscope grid in terms of peak width and maximum value, and NV achieved the best results. In Ref. [6], 13 functions were compared to evaluate sharpness or contrast; self-correlation and NV were found to be the optimal focus measures for fluorescence microscopy applications.

In addition, 16 focus measures on 8000 bright-field images from 10 blood smear and Pap smear samples (which is close to our application domain) were compared in Ref. [1]. The conclusion that image variance exhibits the best

overall performance was provided by this study. Moreover, it suggests that NV is the optimal focus measure for all non-fluorescence microscopy applications. In the same direction, a comprehensive comparison of 18 focus measures was reported in Ref. [11], and NV provided the best overall performance. In Ref. [12], variance presented good discrimination power and a high range of possible values, thus making it an interesting magnitude to determine focus.

DCT-based measure: With regard to DCT application in AF systems, a mechanism that can evaluate the best setting for the lens and the diaphragm by using a DCT proposed in Ref. [13]. DCT-based curves for focused and blurred images were compared in Ref. [14]. An AF method for mobile phones based on the intermediate frequency of a DCT was presented in Ref. [15]. Other recent studies<sup>[16]</sup> concluded that the relation between digital camera focus and a DCT were inseparable.

After evaluating several approaches for using DCT coefficients to assess focus quality, we propose the following novel measure in this letter. For each non-overlapping  $8 \times 8$  image block, we firstly evaluate the sum of the absolute values of half of the AC coefficients and the lower frequency coefficients in zigzag order (left-up part<sup>[23]</sup>) that are sensible to edges but not to noise. Then, we apply a  $3 \times 3$  median filter to the  $8 \times 8$  reduced image of cumulated AC values to reduce the noise effect further. Finally, we obtain the normalized standard deviation of the filtered cumulated AC coefficients.

Combined measure (NV-DCT): We assume that the two focus measures are complementary or independent to a certain degree to be able to combine them into a single approach (NV-DCT). We evaluate the modulus or amplitude of the two-dimensional vector formed by NV-DCT.

In the following paragraphs, we discuss the top five search-based AF algorithms and the proposed searching algorithm (Fig. 1). Search-based algorithms can be divided basically into overall search algorithms (GS, RBS, and HCS) and numeric string algorithms (BS and FS). These algorithms all assume to a certain degree that although the optimal focus measure in passive AF-based search depends on the camera characteristics and the image object being focused or ranged<sup>[17]</sup>, a maximum of the FF generally occurs at the focused lens position<sup>[18]</sup>.

GS: This approach is the most intuitive search-based algorithm. The GS algorithm firstly moves the lens to a predetermined limit position that produces a blurred image. The lens is then moved from the  $z$  axis to the other end by a stepper motor while the FF is computed for each step or position. Finally, the lens returns to the position where the FF corresponds to the optimum focus (i.e., its maximum). The main advantage of this algorithm is that no possibility of falsely obtaining a local maximum exists because all focus positions are examined<sup>[19]</sup>. However, the search time is too long. More importantly, the typical approach of mapping FF values with lens position and moving the lens to the position of the function maximum also lead to imprecision. The stored position may no longer correspond to the best focused image because of the vibration effect in high-magnification midrange setups.

RBS: This algorithm mainly consists of defining rules

based on a priori observations on FF shape to modify the search positions of a GS algorithm, such that positions are closer to the maximum approaches<sup>[20]</sup>. This method accelerates a search at the expense of possibly missing the FF maximum if the rules are wrong. When FF values are mapped to a lens position, this approach can also be affected by vibration.

HCS: Developed for fast searching, HCS<sup>[9]</sup> is also known as the mountain climbing servo<sup>[21]</sup>, modified fast climbing search<sup>[22]</sup>, and peak search<sup>[16]</sup>. Similar to GS, this algorithm firstly moves the lens to a predetermined limit position. Then, it starts searching for and evaluating the FF, assuming that this function is a crescent. As soon as the function decreases, the algorithm stops searching and returns to the position of the maximum. The drawback, as expected, is that the function shape may not be a crescent because of noise.

BS: In this algorithm, which has been used in Ref.[19], the lens is firstly moved to a predetermined limit position. Then, the stepper motor is iteratively moved back and forth to obtain the maximum position, firstly with large motions, and then, with successively smaller ones (Fig. 1), according to a binary series (half larger in every iteration). Although BS is optimal in terms of the number of times that the FF has to be evaluated, the mechanical motion is extensive, thus making this method time consuming<sup>[19]</sup>.

FS: This algorithm is similar to BS except that the series that controls the lens motion amount is a Fibonacci series instead of a binary series<sup>[7]</sup>. We assume a behavior that is similar to BS because the resources required to compute the FF do not depend on the position of the lens.

The proposed algorithm (PA): This algorithm can be regarded as an adaptation of the GS algorithm for the considered domain, with the following differences.

- Instead of resetting the lens to a predetermined out-of-focus position, each slide focusing operation starts at the lens end position where the previous focusing operation has finished (Fig. 1), either in the upper (case I) or lower (case II) position, which is particularly adequate for the sequential capturing of hundreds of images.

- Instead of mapping FF values to the lens position, the PA stores the image that corresponds to the greater FF value. Hence, moving the lens back to any stored position is not necessary to avoid the effect of vibration, which our results show as not negligible.

Our experiment involves testing the 18 AF methods and performing 5 consecutive focusing operations using all the methods for 10 different microscope slides (5 normal and 5 abnormal Pap smear samples). Hence, we obtain 900 focused images and 50 operations for each method.

The results for each focusing operation and method include: 1) the final focused image, which is generally different for each method; 2) the evolution of the  $z$  position of the lens and the FF value as the stepper motor moves the lens. All the collected results can be analyzed in <http://eiiplab.org/QSFTds/>.

The aforementioned evolution for a specific focusing test is illustrated in Fig. 2. Eighteen consecutive focusing operations are shown, i.e., one for each method. The first row uses the NV measure, the second row uses the

DCT-based measure, and the third row uses the combined measure. For each step of the stepper motor, Fig. 2(b) shows the  $z$  position of the lens, whereas Fig. 2(a) shows the value of the FF. Prior to each focusing operation, the lens is in a fixed position ( $z = 1000$ ): the PA automatically moves the lens to the upper position (case I) and scans the  $z$  axis every 150 steps. The other five algorithms require a different number of steps to reach a final focused image (approximately  $z = 1000$ ).

Table 1 lists the quantitative results for the 900 focusing operations. To assess the final quality of the focused

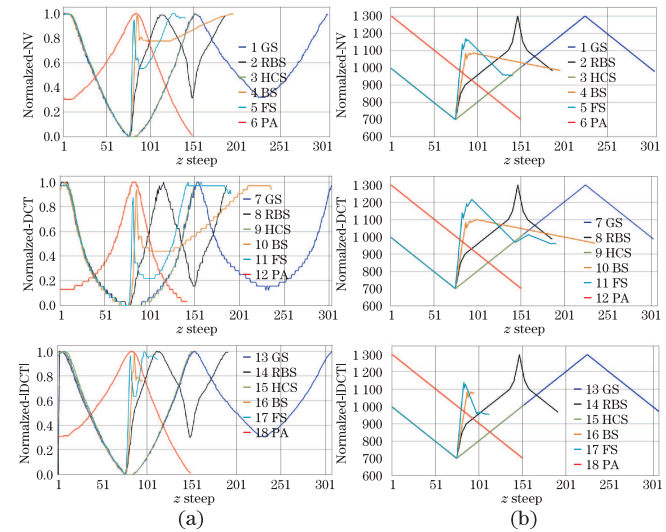


Fig. 2. (Color online) (a) Comparative evolution of the FF and (b) the  $z$  position of the lens for a specific focusing test.

**Table 1. (Color online) Average Results for the 50 Focusing Operations Performed by Each AF Method (The best results are in blue).**

Method	Final Average Value				
	STD $_{\mu}$	STD $_{\sigma}$	NS	$\Delta z$	FF
GS-NV	0.9141	0.1348	316.38	1261.52	0.8408
GS-DCT	0.9239	0.1205	313.52	1250.08	0.8424
GS-NV-DCT	0.8806	0.1549	322.44	1285.76	0.7540
RBS-NV	0.9215	0.1048	192.88	1257.12	0.8522
RBS-DCT	0.9134	0.1183	195.14	1266.16	0.7860
RBS-NV-DCT	0.9170	0.1250	194.5	1263.6	0.8399
HCS-NV	0.8677	0.1721	131.4	521.6	0.6965
HCS-DCT	0.8819	0.1424	137.8	547.2	0.7531
HCS-NV-DCT	0.8054	0.1924	<b>117.04</b>	<b>464.16</b>	0.5187
BS-NV	0.8788	0.1395	156.78	774.96	0.7498
BS-DCT	0.8997	0.1160	154.02	812.82	0.6915
BS-NV-DCT	0.8627	0.1255	<b>123.4</b>	<b>717.7</b>	0.6515
FS-NV	0.9157	0.1286	189.3	1043.76	0.8446
FS-DCT	0.9162	0.1067	189.9	1136.56	0.7730
FS-NV-DCT	0.8615	0.1391	171.26	905.42	0.6490
PA-NV	0.9585	0.0673	150	596	<b>1</b>
PA-DCT	0.9617	0.0492	150	596	<b>1</b>
PA-NV-DCT	<b>0.9657</b>	<b>0.0468</b>	150	596	<b>1</b>

image, we evaluate its standard deviation (normalized for each focusing test with respect to the maximum obtained by the best method). The highest standard deviation provides the best image quality. We also include the mean value ( $STD_{\mu}$ ), deviation ( $STD_{\sigma}$ ), the average number of steps (NS), the length of the path traveled by the lens ( $\Delta z$ ) for each method, and the FF value (normalized for each method with respect to the maximum value of its own FF) for the final acquired focused image.

The data indicate that the PA obtains the most accurate and stable results (Table 1). The proposed DCT measure passes the NV measure and complements it to obtain images with maximum contrast. HCS is the fastest algorithm but also the least accurate. BS is faster than the PA, but less accurate and requires a faster motion of the lens. The PA involves constant motion. Moving the lens back to the  $z$  position that maximizes the FF (NS=1) does not guarantee that the best focused image (observe that GS should obtain NS=1, but it does not) will be obtained because of the aforementioned vibration.

In conclusion, we describe an AF method adapted to capture sequences of focused images automatically from high-magnification microscopes. The method combines two focus measures with a searching algorithm that stores the best focused image as it scans the  $z$  axis with constant velocity. Hence, the proposed method preserves mechanical devices and avoids the vibration effect on high-magnification midrange setups.

This work was supported by the CONACYT/204212 and the DGEST of the Mexican Government under the PROMEP/107.5/10/5417. Special thanks to Dr. Fomuy Woo, CT. Laura Meraz, and Dr. Ma. Guadalupe Hernandez for providing the Pap smear samples.

## References

1. X. Y. Liu, W. H. Wang, and Y. Sun, in *Proceedings of IEEE 28th Annual International Conference on Engineering in Medicine and Biology Society* 4718 (2006).
2. J. M. Geusebroek, F. Cornelissen, A. W. Smeulders, and H. Geerts, *Cytometry* **39**, 1 (2000).
3. M. E. Plissiti, C. Nikou, and A. Charchanti, *IEEE Trans. Inform. Technol. Biomed.* **15**, 233 (2011).
4. J. Luo, L. Sun, K. Wu, W. Chen, and L. Fu, *Chin. Opt. Lett.* **8**, 580 (2010).
5. C. H. Chang and C. S. Fuh, "Auto Focus Using Adaptive Step Size Search and Zoom Tracking Algorithm", Master Thesis (National Taiwan University, 2005).
6. A. Santos, C. Ortiz de Solorzano, J. J. Vaquero, J. M. Pena, N. Malpica, and F. Del Pozo, *J. Microsc.* **188**, 264 (1997).
7. X. Y. Liu, W. H. Wang, and Y. Sun, *J. Microsc.* **227**, 15 (2007).
8. C. Y. Chen, R. C. Hwang, and Y. J. Chen, *Applied Soft Computing* **10**, 296 (2010).
9. K. S. Choi, J. S. Lee, and S. J. Ko, *IEEE Trans. Consum. Electron.* **45**, 820 (1999).
10. F. C. Groen, I. T. Young, and G. Lighthart, *Cytometry* **6**, 81 (1985).
11. Y. Sun, S. Duthaler, and B. J. Nelson, in *Proceedings of IEEE/RSJ International Conference on Intelligent Robots and Systems* 70 (2005).
12. P. R. Fernández, J. L. Lázaro, A. Gardel, Á. E. Cano, and I. Bravo, *Sensors* **10**, 47 (2010).
13. J. Baina and J. Dublet, in *Proceedings of the Fifth International Conference on Image Processing and its Applications IET*, 232 (1995).
14. M. Charfi, A. Nyeck, and A. Tossier, *Electron. Lett.* **27**, 1233 (1991).
15. S. Y. Lee, S. S. Park, C. S. Kim, Y. Kumar, and S. W. Kim, in *Proceedings of IEEE Conference on Consumer Electronics* 67 (2006).
16. X. Xu, Y. Wang, J. Tang, X. Zhang, and X. Liu, *Sensors* **11**, 8281 (2011).
17. M. Subbarao and J. K. Tyan, *IEEE Trans. Pattern Anal. Mach. Intell.* **20**, 864 (1998).
18. K. C. Lin, *J. Electron. Imag.* **19**, 023012 (2010).
19. M. J. Russell, A. Bester, and T. S. Douglas, in *Proceedings of the Sixteenth Annual Symposium of the Pattern Recognition Association of South Africa* 183 (2005).
20. N. Kehtarnavaz and H. J. Oh, *R. Time Imag.* **9**, 197 (2003).
21. K. Ooi, K. Izumi, M. Nozaki, and I. Takeda, *IEEE Trans. Consum. Electron.* **36**, 526 (1990).
22. J. He, R. Zhou, and Z. Hong, *IEEE Trans. Consum. Electron.* **49**, 257 (2003).
23. Q. Zhao, X. Luo, N. Zhou, and J. Wu, *Chin. Opt. Lett.* **10**, 11006 (2012).